<div align="center">**Responses to reviewer 3#'s comments point by point**</div>

MS No.: essd-2022-436

Title: A grid dataset of leaf age-dependent LAI seasonality product (Lad-LAI) over tropical and subtropical evergreen broadleaved forests

Author(s): Xueqin Yang et al.

General Comments of Reviewer 3#:

This paper introduces a novel dataset of age-dependent LAI for tropical and subtropic evergreen forests. Such a dataset is highly valuable and much in need to understand the dynamics of tropical canopy structure under climate change and improve the robustness of Earth System Models in reconstructing past dynamics and projecting future scenarios. The study estimated three LAI age cohorts based on a neighbor-based decomposition model and SIF-derived GPP data. The seasonality of leaf demography and its spatial variations is evaluated against ground-based measurements, and satellite observations, and analyzed with regard to other independent studies from climate controls. Results suggested a robust representation of the spatial variability in seasonality, which will be useful for improving Earth System Models. Overall, I find the dataset to be valuable and significant. I especially appreciate the authors' efforts in collecting and synthesizing ground-based observations globally to evaluate the products. However, I have some concerns regarding the robustness of the neighbor-based decomposition approach, the absence of evaluation regarding interannual dynamics, and the uncertainties in GPP estimations. I hope the authors will consider these points and provide further clarification in their responses and/or revisions. Please find my major comments and minor for clarification below.

Response: Thanks so much for the constructive comments and suggestions regarding our manuscript. We have revised the manuscript thoroughly regarding the robustness of the neighbor-based decomposition approach, the absence of evaluation regarding interannual dynamics, and the uncertainties in GPP estimations as commented by reviewer, to

(1) To prove the robustness of the neighbor-based decomposition approach, we compared the Lad-LAI products generated based 2*2 neighbor pixels and 4*4 neighbor pixels. The seasonality and magnitudes of LAI of young, mature and old leaf cohorts are consistent between the two datasets (Figure R4, R5) (See responses to Comment 1).

(2) To evaluate the interannual dynamics of Lad-LAI, we could only find one ground site (Barrocolorado site in Panama) with time-series camera-based phenological imageries. Results showed that Lad-LAI could detect the interannual dynamic but more in situ observations are in need to test the robustness (Figure S3) (See responses to Comment 2).

(3) To test the uncertainties caused by the GPP estimation, we added two GPP products, i.e., GOSIF-derived GPP and FLUXCOM GPP for comparisons. Results showed that the Lad-LAI generated from SIF-derived GPP show highest consistent with the in situ observed LAI seasonality of different leaf age cohorts (Figure R6-R10). (See responses to Comment 3).

Major Comments:

Comment 1: The approach using spatially adjacent GPP information to solve the leaf age composition is interesting but needs more justification on its robustness. With four observations (from four neighboring pixels) to solve three unknowns (LAI cohorts), the system does not have much space or tolerance for observation uncertainties (that is GPP, please see a related comment below). I suggest providing goodness-of-fit metrics from the least squares to evaluate the model performance. However, this still may not be informative due to a limited number of observations and lack of variations between the neighboring cells. Ideally, one solution would be to include more observations (for example, by increasing the number neighboring pixels from 4 to 8) to improve the robustness and accuracy of the models, but that also means a decrease in the spatial resolution of the product.

Response: Thanks for nice suggestion in testing the robustness of the neighbor-based decomposition approach. Following your comments, we have increased the number of adjacent pixels from 4 (2*2) to 16 (4*4) to produce another version of Lad-LAI products with spatial resolution of 0.5-degree. Then, we compared the monthly LAI_{young}, LAI_{mature}, LAI_{old} between the two datasets in the 8 clustered regions. Results showed that the seasonality of LAI_{young}, LAI_{mature}, LAI_{old} are highly consistent in the 8 clustered regions (Figure R4, R5), and the correlation coefficients of LAI_{young}, LAI_{mature}, LAI_{old} between the two datasets are $R_{young}= 0.63$, $R_{mature}= 0.68$, $R_{old}= 0.95$, respectively, implying the robustness of neighbor-based decomposition approach in decomposing the monthly LAI_{young}, LAI_{mature} and LAI_{old} from the monthly GPP using Equation 1.
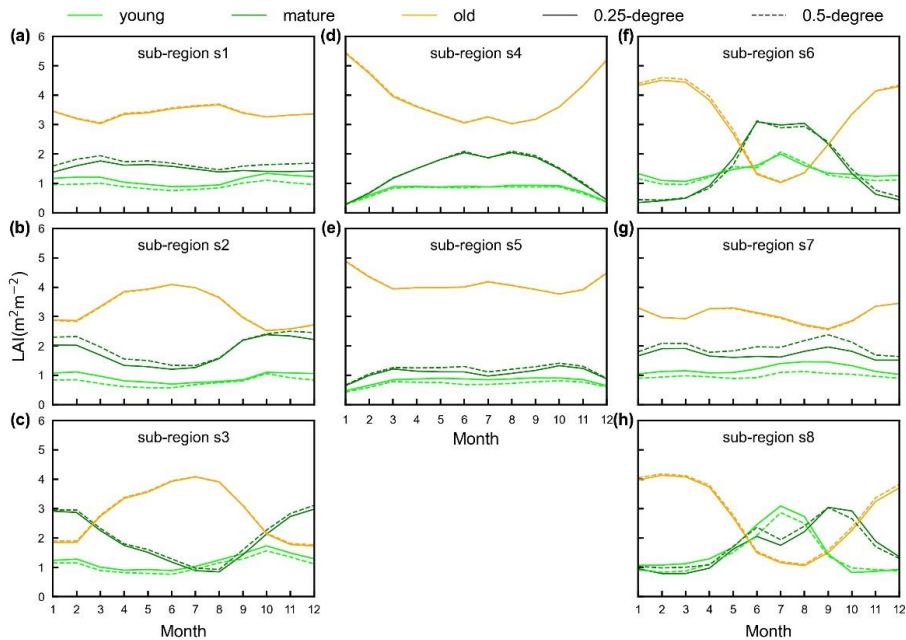

Figure R4. The seasonality of LAI_{young}, LAI_{mature}, LAI_{old} between 0.25-degree and 0.5-degree LAI cohort datasets in the 8 clustered regions. The limegreen color represents LAI_{young}; green color represents LAI_{mature}; and orange color represents LAI_{old}. The solid lines represent 0.25-degree dataset and the dashed lines represent 0.5-degree datasets.
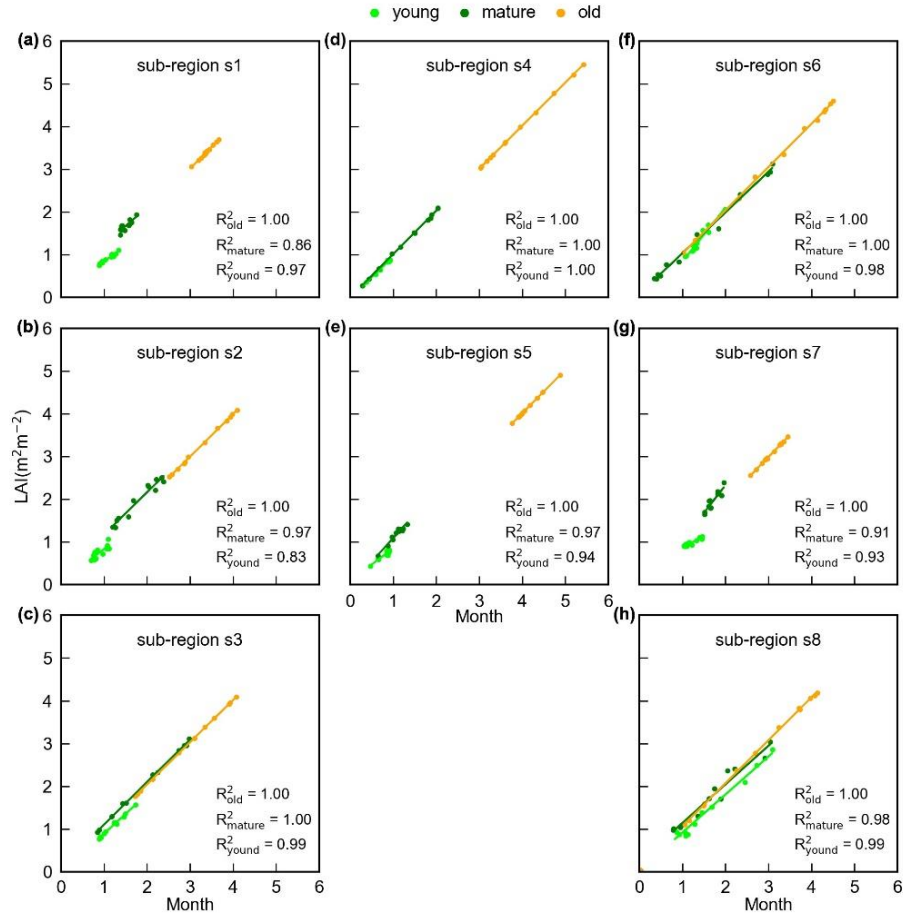
Figure R5. *The scatterplot of 0.25-degree LAI$_{young}$, LAI$_{mature}$, LAI$_{old}$ against 0.5-degree LAI cohort datasets in the 8 clustered regions.*

Comment 2: While the age-dependent LAI product is produced at monthly time steps over 2001-2018, it has only been validated and evaluated in terms of its LAI seasonality (i.e. multi-year average climatology). The reliability and usefulness of this product in representing interannual variabilities of leaf demography are highly uncertain. Thus, I strongly encourage the authors to evaluate the interannual temporal dynamics, even if only limited, since ground observations are often insufficient. The reliability of this product in terms of representation seasonality vs. interannual variabilities should be explicitly stated in the abstract, and thoroughly discussed in the main text, to prevent misuse of the dataset. I also suggest providing LAI cohorts seasonality as the main product, and the temporal dynamics as a supplementary dataset with a clear note of usage provided along with the product.

Response: *We appreciate for the reviewer's comment. We totally agree that it is important to evaluate the interannual temporal dynamics of the age-dependent LAI product. As said by the reviewer that the time-series ground observations are very limited, we could only find one ground site (Barrocolorado site in Panama) with time-series camera-based phenological imageries, to evaluate the interannual dynamics of Lad-LAI. Results showed that Lad-LAI could detect the interannual dynamic. The R^2 of the timeseries of LAI$_{young}$, LAI$_{mature}$, LAI$_{old}$ between the two datasets are 0.30, 0.41, 0.24,*

respectively (Figure S3). However, more in situ observations are in need to test the robustness. We thoroughly discussed the timeseries variability of LAI cohort dataset. We presented the temporal variations of LAI_{young}, LAI_{mature}, LAI_{old} across 8 sub-regions classified by the K-means clustering analysis (Figure S4). The results demonstrated a consistent pattern of interannual variation, implying potential good capability of detecting abnormal events (e.g. subregion s7).
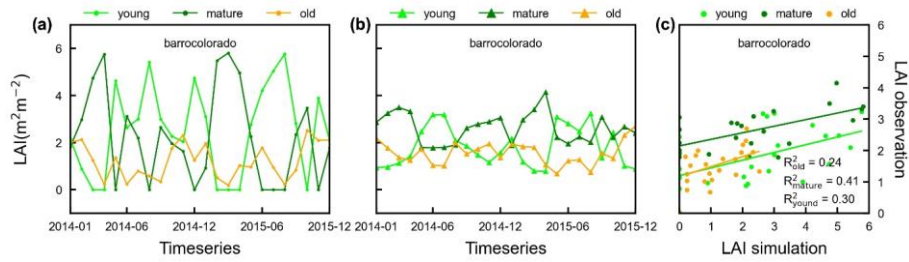

Figure S3. *Timeseries of simulated LAI_{young}, LAI_{mature}, and LAI_{old} in comparison with observed data at Barrocolorado site in Panama. (a) simulations LAIs; (b) observation LAIs; and (c) scatterplots between simulated and observed LAIs.*
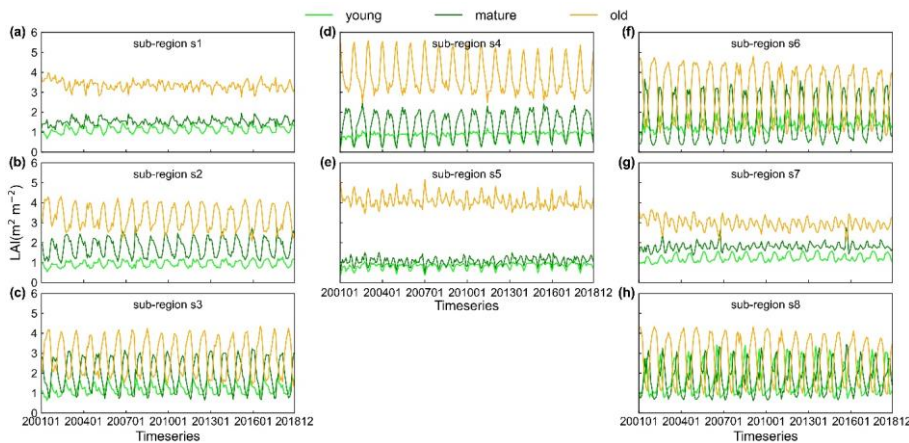

Figure S4. *Timeseries of simulated LAI_{young}, LAI_{mature}, and LAI_{old} in 8 sub-regions classified by the K-means clustering analysis. Limegreen represents LAI_{young}; green represents LAI_{mature}; and orange represents LAI_{old}.*

*We also agree with the suggestion to provide the LAI cohorts seasonality as the main product and the temporal dynamics as a supplementary dataset. In addition, we provided information of data quality control (QC) for the Lad-LAI product to prevent data misuse. In the QC system (**Table S6**), data quality is divided into four levels: level 1 represents the highest quality; level 2 and level 3 represent good and acceptable quality, respectively; and level 4 warns to be used cautiously. This QC product is generated according to the goodness of fit (residual sum of squares, RSS) (Melgosa et al., 2008, 2011) obtained from the constrained least-squares method used to estimate derive monthly Lad-LAI data. Results showed that more than 92.62% of pixels are with QC at best and gool levels and only less than 5.62% are with QC at level 4.*

Table S6 *Information of data quality control (QC) for the Lad-LAI product*

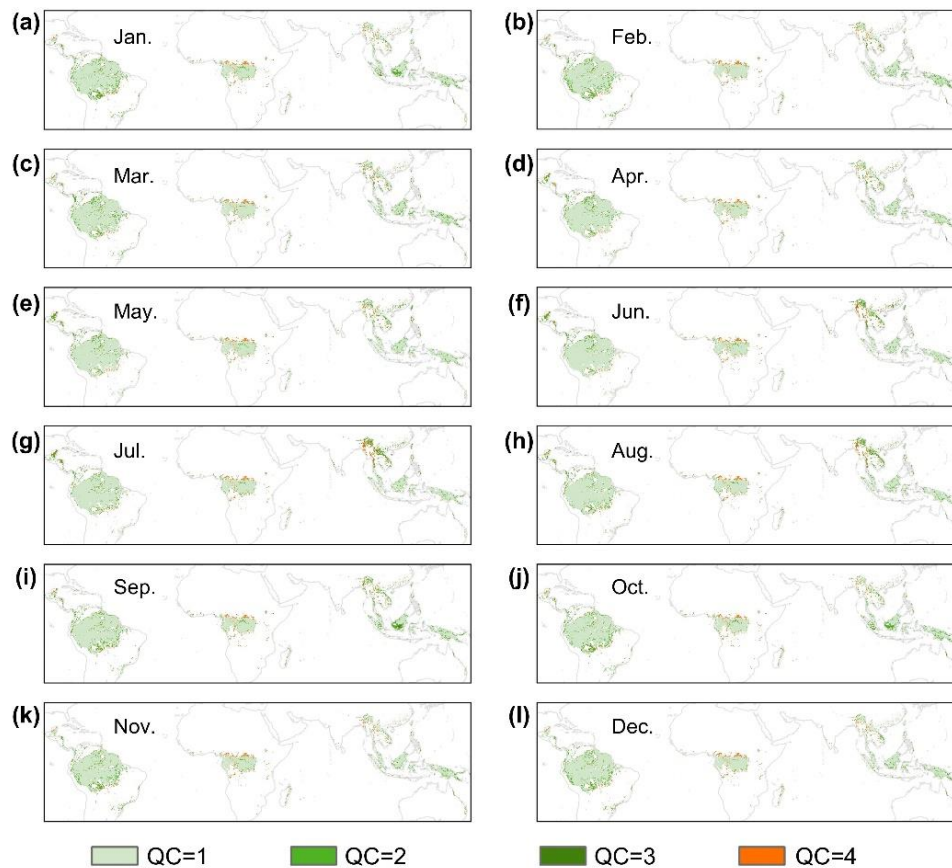| QC class	QC value	residual sum of squares (RSS)
Best	1	0-1
Good	2	1-4
Acceptable	3	4-9
Cautious use	4	>9

Figure S8. *Spatial patterns of seasonal QC datasets.*

Comment 3: SIF-GPP relationships used to estimate GPP in this study were based on only four sites with ground observations, that may not fully represent the tropical areas over the globe. Therefore, GPP estimations from SIF are subject to high uncertainties with possibly large biases. Given that the analytical approach used to solve does not consider uncertainties, the impact of GPP estimation uncertainties on age-dependent LAI estimates should be carefully discussed.

Response: Thank you for the valuable comment. To test the uncertainties caused by the GPP estimation, we added two more GPP products, i.e., GOSIF-derived GPP and FLUXCOM GPP, to produce two versions of Lad-LAI products, for comparisons.

Firstly, we need to clarify that the overall regression slope of 15.343 in the 8-day between GPP and RTSIF represent over the regional average (Chen et al., 2022), not from SIF-GPP relationships based on only four sites with ground observations. Chen et al. (2022) established the linear relationship between RTSIF and GPP using 76 sites

GPP data from the FLUXNET 2015 Tier 1 dataset in both 8-day and annual timescale (Fig. 8 in Chen et al. (2022)), indicating that RTSIF is tightly related to GPP. According to Chen et al. (2022), RTSIF was in good agreement with FLUXNET GPP for almost all biomes at the 8-day timescale, indicating strong SIF-GPP correlations for different biomes.

Second, to test the uncertainties of different SIF-GPP relationship on our analyses, we used the GOSIF-derived GPP products to produce another version of Lad-LAI. The GOSIF-derived GPP are generated based on various SIF-GPP relationships for the period from 2000 to 2020. According to Li and Xiao (2019), at site-level, the universal and biome-specific SIF-GPP relationships are established based on SIF soundings from OCO-2 and GPP data from 64 EC sites. And at grid cell level, a SIF-GPP relationship is established based on 0.05° GOSIF data and tower GPP. All of these SIF-GPP relationships with different forms (universal and biome-specific, with and without intercept) at both site and grid cell levels performed well in estimating GPP globally. We also used an independent GPP product—FLUXCOM GPP products to produce a third version of Lad-LAI. The FLUXCOM GPP are estimated from machine learning to merge carbon flux measurements from FLUXNET eddy covariance towers with remote sensing and meteorological data. We compared the seasonality of three GPP datasets in 8 sub-regions classified by the K-means clustering analysis. Results showed that the GPP seasonality are mostly consistent in 8 sub-regions (Figure R6).
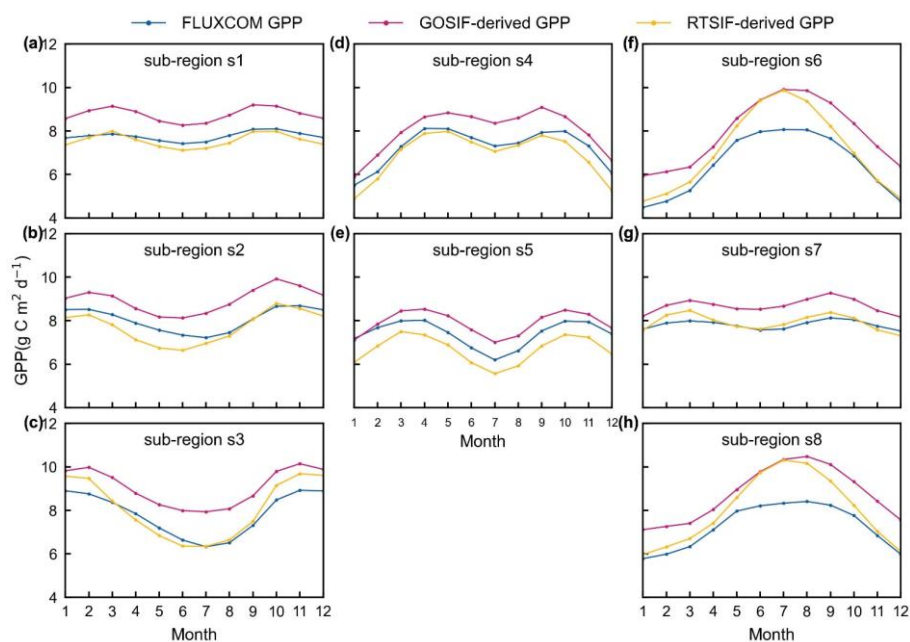

Figure R6. Seasonality of RTSIF-derived GPP (yellow lines), GOSIF-derived GPP (pink lines) and FLUXCOM GPP (blue lines) datasets in 8 sub-regions classified by the K-means clustering analysis. (a-c) South American; (d-e) Congo; (f-h) tropical Asia.

For the three versions of Lad-LAI products, eight camera-based observation sites are used for compare the accuracy of the corresponding simulated LAI cohorts (Figure R7, R8, R9). We also compared the seasonal variability between three versions products

in 8 sub-regions classified by the K-means clustering analysis (Figure R10). Results showed that the Lad-LAI generated from RTSIF-derived GPP show highest consistent with the in situ observed LAI seasonality of different leaf age cohorts (Figure R7, R8, R9). The highest accuracies of the seasonality of LAI_{young}, LAI_{mature}, LAI_{old} between the observed sites and the three datasets are all come from the Lad-LAI generated from RTSIF-derived GPP, $R^2_{young\ vs\ RTSIF\text{-}derived\ GPP}= 0.41$, $R^2_{mature\ vs\ RTSIF\text{-}derived\ GPP} = 0.62$, $R^2_{old\ vs\ RTSIF\text{-}derived\ GPP} = 0.63$, respectively.

In general, three versions of Lad-LAI products all performed well in 8 sub-regions with the consistent seasonal variability (Figure R10). In subregion s3, s6 and s8 keep the high consistent seasonal variability among three products, particularly. But the Lad-LAI generated from GOSIF-derived GPP performs a little poor in Amazon (sub-region s1, s2 and s3).
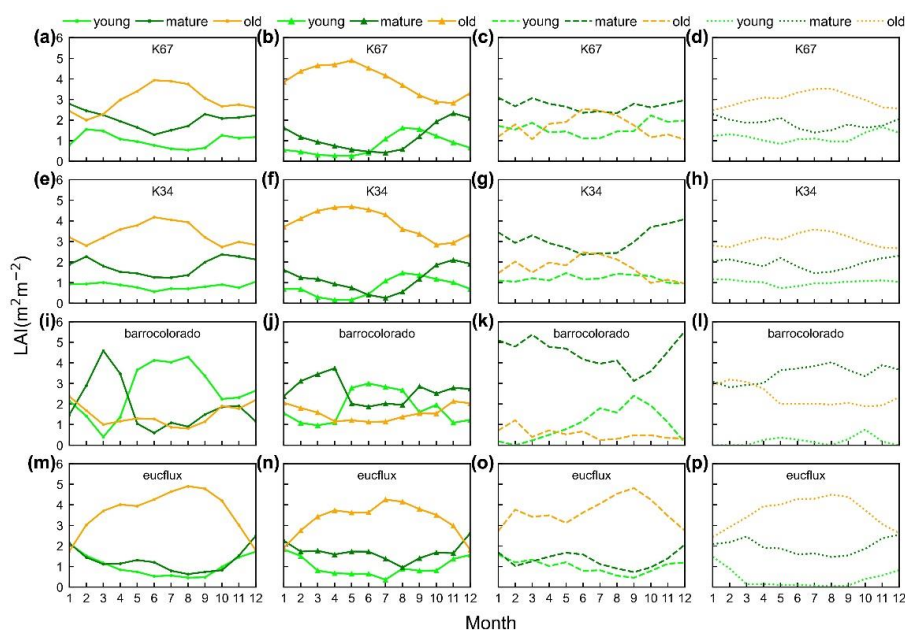

Figure R7. *Seasonality of simulated LAI_{young}, LAI_{mature}, and LAI_{old} in comparison with observed data at 4 sites in South American. (panels a, e, i and m) simulated LAIs from RTSIF-derived GPP; (panels b, f, j and n) camera-based observed LAIs; (panels c, g, k and o) simulated LAIs from GOSIF-derived GPP; and (panels d, h, l and p) simulated LAIs from FLUXCOM GPP.*
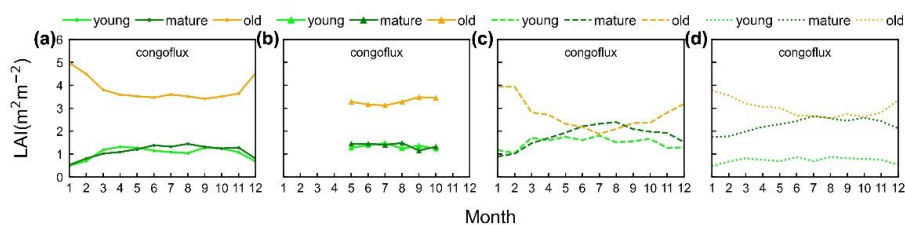

Figure R8. *Seasonality of simulated LAI_{young}, LAI_{mature}, and LAI_{old} in comparison with observed data at one site in Congo. (a) simulated LAIs from RTSIF-derived GPP; (b) camera-based observed LAIs; (c) simulated LAIs from GOSIF-derived GPP; and (d) simulated LAIs from FLUXCOM GPP.*
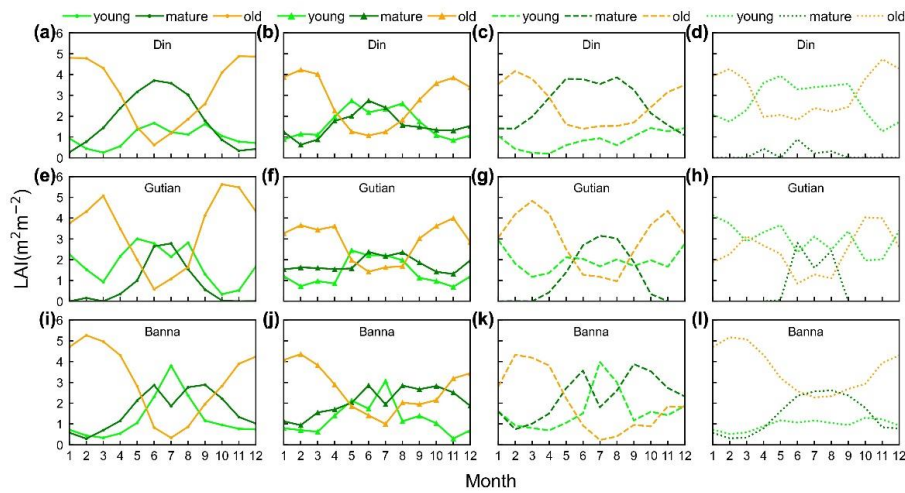
Figure R9. *Seasonality of simulated LAI$_{young}$, LAI$_{mature}$, and LAI$_{old}$ in comparison with observed data at 3 sites in tropical Asia. (panels a, e and i) simulated LAIs from RTSIF-derived GPP; (panels b, f and j) camera-based observed LAIs; (panels c, g and k) simulated LAIs from GOSIF-derived GPP; and (panels d, h and l) simulated LAIs from FLUXCOM GPP.*
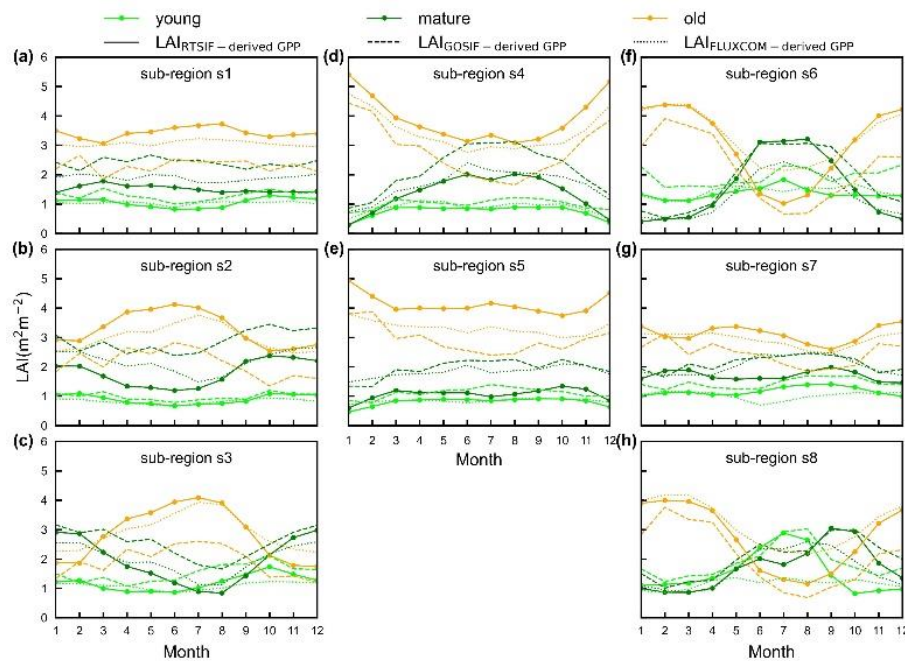

Figure R10. *Seasonality of simulated LAI$_{young}$, LAI$_{mature}$, and LAI$_{old}$ from three version products in 8 sub-regions classified by the K-means clustering analysis. Limegreen represents LAI$_{young}$; green represents LAI$_{mature}$; and orange represents LAI$_{old}$.*

Comment 4: Please note that evaluation against EVI is not entirely independent, since the RT-SIF dataset was a reconstruction from MODIS NBAR surface reflectance data. The manuscript needs improvements in language and grammar. I suggest carefully revising it to improve clarity.

Response: *Thanks for pointing this out. To be cautious, we have removed the statements of using "independent" in the revised manuscript. For the capability of using EVI as a*

proxy for validating the seasonality young and mature leaves, Huete et al. (2006) found that Amazon rainforests green-up in dry season due to sunlight derive the synchronous canopy leaf turnover the young and mature leaves. And de Moura et al. (2017) compared tower and MODIS data with leaf flush and LAI from young to old leaves, and found an EVI increase toward September that closely tracked the modeled LAI of young/mature leaves (3–5 months). The MODIS EVI products are very sensitive to changes in NIR reflectance (Galvão et al., 2011) and young and mature leaves also could reflect more near-infrared (NIR) light than the older leaves replaced (Toomey et al., 2009). We have added such explanation in the new version.

For the improvements in language and grammar of the manuscript, we totally rewrote the Introduction (see responses to Comment 8 and Review 2# Comment 4), largely revised the Study area and data sections (see responses to Review 2# Comment 5). Finally, we also asked a company to polish our English language, including grammar, syntax, and sentence structure, to improve the readability of the manuscript.

Specific Comments:

Abstract:

Comment 5: Please specify the temporal span, temporal and spatial resolution of the LAI product.

Response: *Thanks for your comment. We revised it as suggested. The abstract revised as follows: "Here, we simplified the canopy leaves of TEFs into three age cohorts, i.e., young, mature and old one, with different photosynthesis capacity ($V_{c,max}$) and proposed a novel neighbor-based approach to develop a first monthly grid dataset with 0.25-degree spatial resolution of leaf age-dependent LAI product (**referred to as Lad-LAI**) during 2001-2018 over the continental scale from satellite observations of sun-induced chlorophyll fluorescence (SIF) that was reconstructed from MODIS and TROPOMI (the TROPOspheric Monitoring Instrument) as a proxy of leaf photosynthesis."*

Comment 6: L36: It should be noted that this is a SIF dataset that was reconstructed from MODIS and TROPOMI to avoid confusion.

Response: *Thanks for your reminder. We have corrected it. (See responses to Comment 5)*

Comment 7: L40-41: Since the RTSIF is reconstructed from MODIS surface reflectance data, the evaluation against EVI is not precisely "independent".

Response: *Thanks again. We have removed the statements of using "independent" in the revised manuscript.*

Introduction:

Comment 8: L103: The last paragraph of the Introduction should be shortened with a brief summary of the method and findings.

Response: *Done as suggested. We have shortened this paragraph with a brief summary*

of the method and findings as follows.

*"To fill the research gap, this study aims to produce a grid dataset of leaf age-dependent LAI seasonality product (Lad-LAI) at the continental scale over the TEF biomes from 2001 to 2018. For this purpose, we simplified that canopy GPP was composed of three parts that are produced from young, mature and old leaves, respectively; and based on this assumption, GPP was expressed as a function of the sum of the product of each LAI cohort (i.e., young, mature and old leaves, denoted as LAI_{young}, LAI_{mature}, and LAI_{old}, respectively) and corresponding net CO_2 assimilation rate (An, denoted as An_{young}, An_{mature}, and An_{old} for young, mature and old leaves, respectively) (**Equation 1**). Then, we proposed a novel neighbor-based approach to derive the values of three LAI cohorts. It is hypothesized that forests in adjacent four cells in the grid map exhibit consistent magnitude and seasonality of GPP, LAI_{young}, LAI_{mature}, and LAI_{old}. By applying **Equation 1** to each of the four selected cells, we combined the four equations to derive the three LAI cohorts using a linear least-squares with constrained method. An is calculated using the Farquhar-von Caemmerer-Berry (FvCB) leaf photochemistry model (Farquhar et al., 1980); and GPP is linearly derived from an arguably better proxy—TROPOMI (the TROPOspheric Monitoring Instrument) Solar-Induced Fluorescence (SIF) calibrated by eddy covariance GPP data (**See Methods for details**). This grid dataset of three LAI cohorts provides new insights into tropical and subtropical phenology with more details of sub-canopy level of leaf seasonality in different leaf age cohorts and will be helpful for developing accurate tropical phenology model in ESMs."*

Method:

Comment 9: L132-133: How much are the spatial variations in the constant LAI value?

Response: *We analyzed the measured LAI values mentioned in other studies and found there are slightly spatial and seasonal variations in totally LAI (Figure R1, R2). A constant total LAI value (around 6.0) can be used for most evergreen broadleaf forests.*
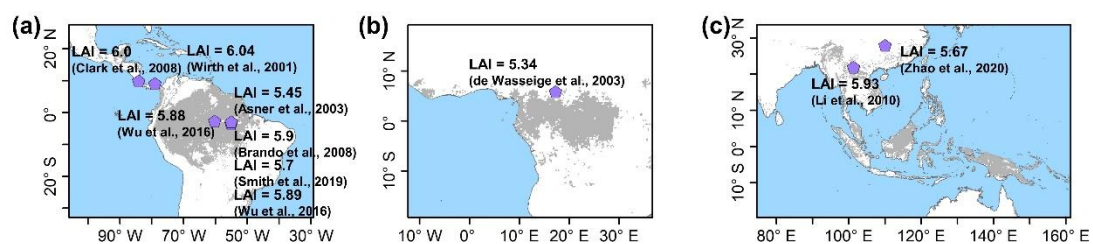

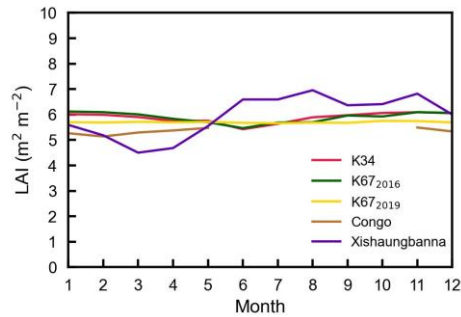**Figure R1.** *The measured LAI sites distribution map.*

Figure R2. *The seasonality of observed total LAI values from other studies.*

Comment 10: L147-168: Using GPP-SIF relationships based on only four sites is suspect to extrapolation issues over the entire areas.

Response: *We apologies for this mistake describe. We have corrected it. The revised as follows: "The GPP is derived from SIF (denoted as RTSIF-derived GPP) using a linear regression model (see sect. 2.2) based on the relationship between RTSIF and EC-observed GPP from 76 sites (Chen et al., 2022)."*

Comment 11: L155: VPD data sources are different between Table S3 and Figure 2. ERA5-Land is at 0.1 degree instead of 0.05 deg? Can you double check?

Response: *Thank you for your attention to detail. VPD datasets was calculated from ERA Interim datasets.*

Comment 12: L175: Could you please provide the GPP-SIF relationship equation and overall goodness-of-fit?

Response: *Yes. The overall regression slope of 15.343 in the 8-day between GPP and RTSIF actually represent the regional average, which was provided by Chen et al., 2022, not from SIF-GPP relationships based on only four sites with ground observations. Chen et al. (2022) explored the relationship between RTSIF and GPP using 76 sites GPP data from the FLUXNET 2015 Tier 1 dataset, and found that there is a linear relationship between RTSIF and GPP in both 8-day and annual timescale (Fig. 8 in Chen et al. (2022)), indicating that RTSIF is tightly related to GPP. And they also reported RTSIF was in good agreement with FLUXNET GPP for almost all biomes at the 8-day timescale, indicating strong SIF-GPP correlations for different biomes.*

Comment 13: L270-271: Note that the RTSIF product is reconstructed from MODIS using the short-term TROPOMI data as a training set. Therefore, the evaluation against EVI is not independent.

Response: *Yes, we agree with your comment and appreciate your reminder. We will use more accurate descriptions in the revised manuscript.*

Comment 14: L273: Can you please elaborate on how EVI reflects young and mature leaves, not old ones?

Response: *Previous studies which used independent satellite observations from lidar and optical sensors reported a consistent phenomenon — dry-season greening in*

Amazon forests (Saleska et al., 2007; Huete et al., 2006; Myneni et al., 2007). And one of the potential biophysical mechanisms of this seasonal greening in Amazon forests is synchronous canopy leaf turnover (Huete et al., 2006; Brando et al., 2010; Doughty et al., 2008) and young leaves flushing. The young leaves could reflect more near-infrared (NIR) light than the older leaves replaced (Toomey et al., 2009). The MODIS EVI products are very sensitive to changes in NIR reflectance (Galvão et al., 2011). As results, when MODIS EVI products were corrected for these effects using the Multi-Angle Implementation of Atmospheric Correction Algorithm (MAIAC), an EVI increase toward September that closely tracked the modeled LAI of young/mature leaves (3–5 months) (de Moura et al., 2017).

Comment 15: L274: Specify MSD

Response: *MSD is the abbreviation for Mean Squared Deviation. The analysis of MSD clearly identified the simulation vs. measurement contrasts with larger deviation than others; the correlation–regression approach tended to focus on the contrasts with lower correlation and regression line far from the equality line. It was shown results of the MSD-based analysis were easier to interpret than those of regression analysis. This is because the three MSD components are simply additive and all constituents of the MSD components are explicit. This approach will be useful to quantify the deviation of calculated values obtained with this model from measurements. We have added more details to specify MSD in revision.*

Comment 16: Figure S1: the figure is too blur to read.

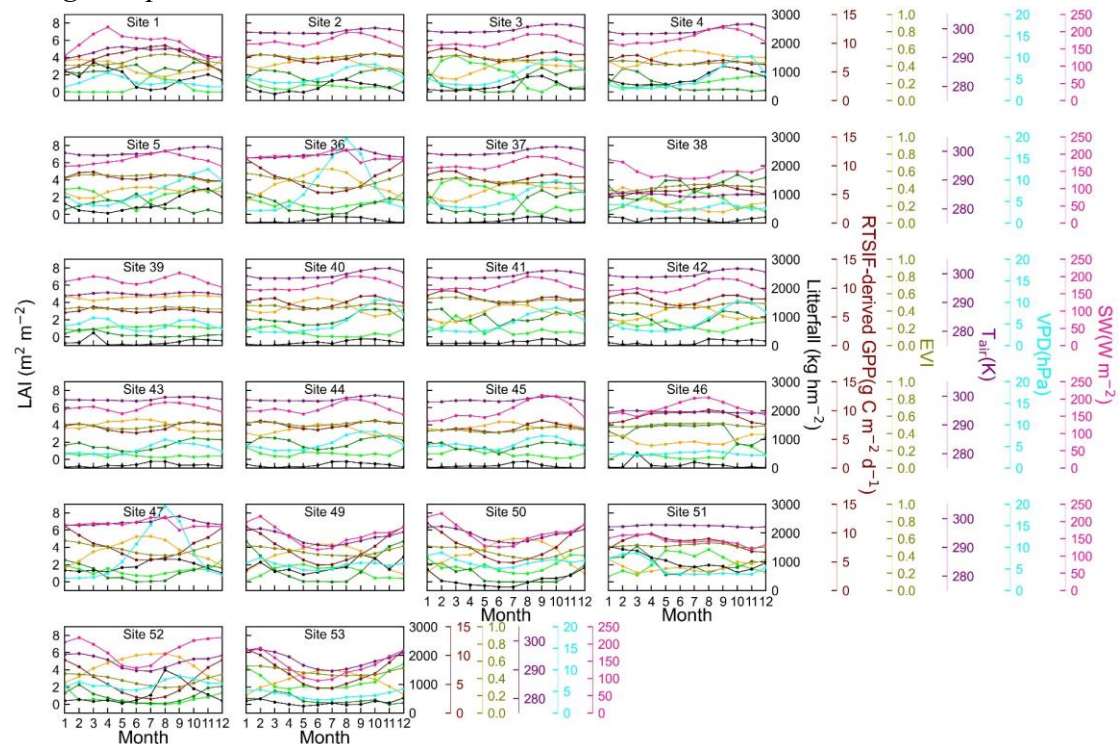**Response:** *We divided into 3 classes for all those sites by region, South American, Congo, tropical Asia. Thanks.*

Figure S5. *Seasonality of LAI$_{young}$, LAI$_{mature}$, LAI$_{old}$, litterfall, EVI, RTSIF-derived GPP,*
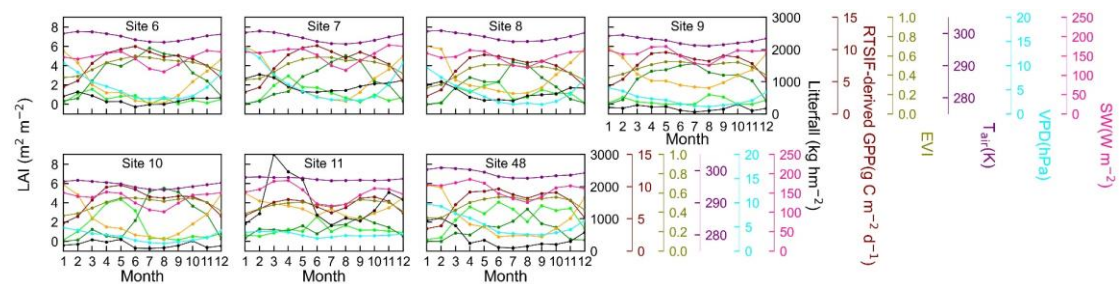
T_{air}, VPD and SW at South American 22 sites.

Figure S6. *Seasonality of LAI_{young}, LAI_{mature}, LAI_{old}, litterfall, EVI, RTSIF-derived GPP, T_{air}, VPD and SW at Congo 7 sites.*
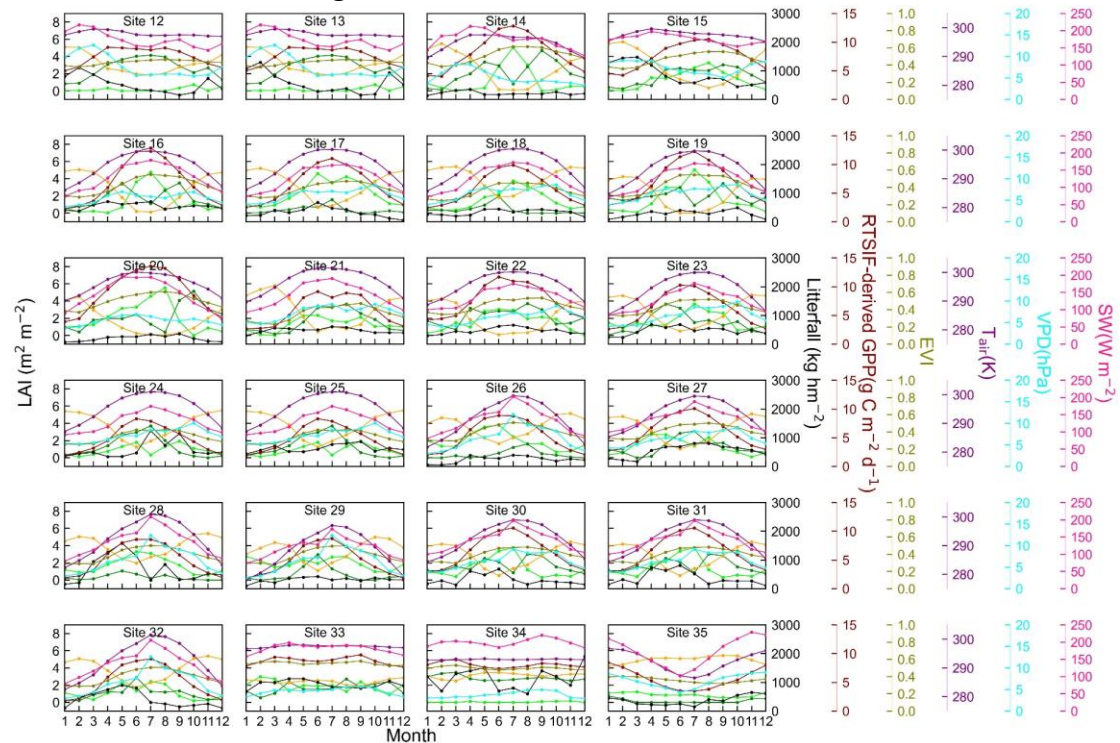

Figure S7. *Seasonality of LAI_{young}, LAI_{mature}, LAI_{old}, litterfall, EVI, RTSIF-derived GPP, T_{air}, VPD and SW at tropical Asia 24 sites.*

Comment 17: L326: Please specify which variable (x,y) is estimated or observed.
Response: *Thanks. In original manuscript L326, in general, simulated value for LAI is denoted as X, and measured value is denoted as Y. Specifically, in original manuscript L351-355, to quantify the sites accuracy, MSD was calculated by X as estimated and Y as observed. In original manuscript Figure 8, to calculate MSD ($LAI_{young+mature}$ & EVI), X is $LAI_{young+mature}$ and Y is EVI.*

Result:
Comment 18: Figure 5: It's not clear which is estimated versus observed data.
Response: *Thanks for your comments. We have clarified in Figure 5 caption that the left column represents the simulated values, the middle column represents the observed values, and the right column shows the scatterplot.*
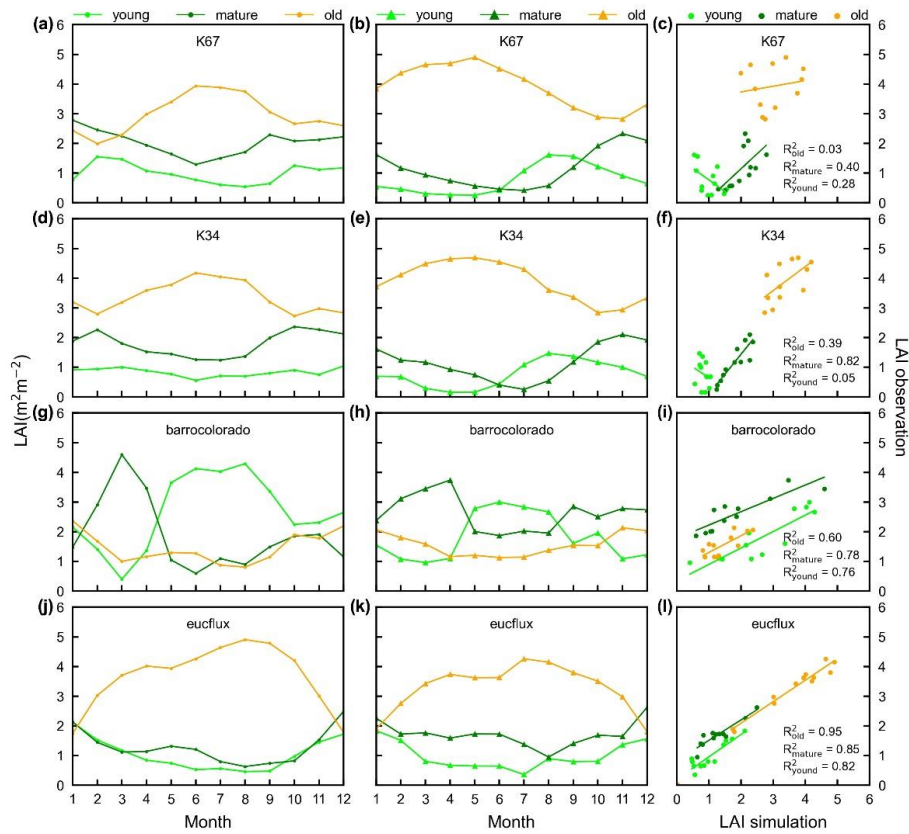
Figure 3. *Seasonality of simulated LAI_young, LAI_mature, and LAI_old in comparison with observed data at 4 sites in South American. (panels a, d, g and j) simulated LAIs; (panels b, e, h and k) observed LAIs; (panels c, f, i and l) scatterplots between simulated and observed LAIs. Limegreen dots are LAI_young; green dots are LAI_mature; orange dots are LAI_old.*

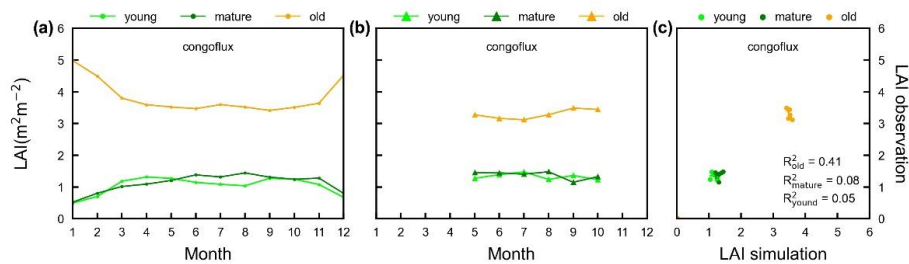***Figure 4***. *Seasonality of simulated LAI_young, LAI_mature, and LAI_old in comparison with observed data at one site in Congo. (a) simulated LAIs; (b) observed LAIs; and (c) scatterplots between simulated and observed LAIs. Limegreen dots are LAI_young; green dots are LAI_mature; orange dots are LAI_old.*

Figure 5. *Seasonality of simulated LAI$_{young}$, LAI$_{mature}$, and LAI$_{old}$ in comparison with observed data at 3 sites in tropical Asia. (panels a, d and g) simulated LAIs; (panels b, e and h) observed LAIs; (panels c, f and i) scatterplots between simulated and observed LAIs. Limegreen dots are LAI$_{young}$; green dots are LAI$_{mature}$; orange dots are LAI$_{old}$.*
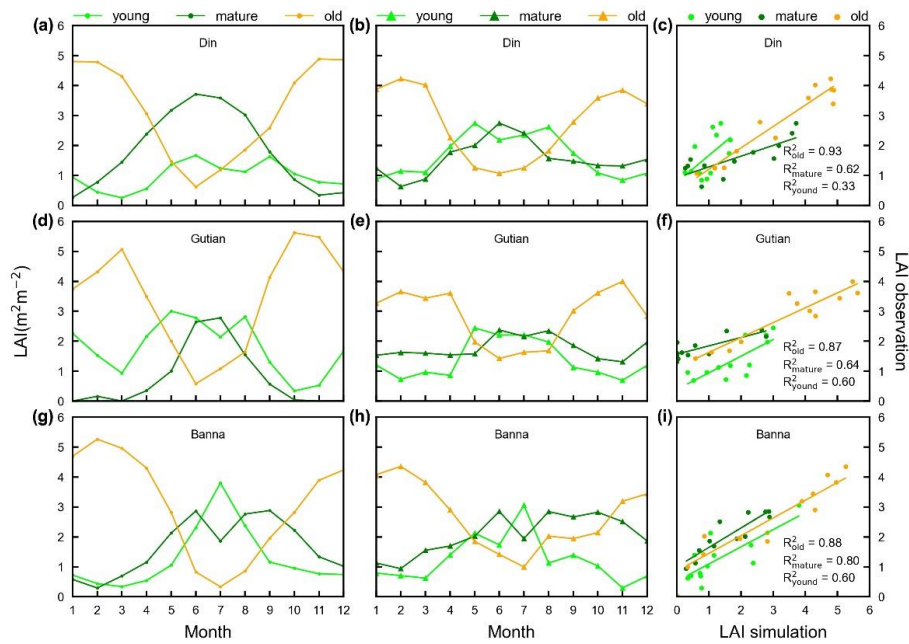
Comment 19: L355-357: This sentence is a bit unclear. Can you elaborate on the "trade-off"?

Response: *Yes. In tropical and subtropical evergreen broadleaved forests, trees adapt their leaf phenology to avoid unfavorable environments such as limited light and water, and maximize their growth rate (Kikuzawa 1995; Vico et al., 2015). And the "trade-off" between the phenology of mature and old leaves means that these forests exhibit complex leaf shedding and rejuvenation strategies in response to moisture and light availability, and these strategies depend on soil water, atmospheric vapor pressure deficit, and incoming solar radiation. Specifically, leaf shedding in the dry season may be an adaptive response to soil water deficits (Asner et al., 2010; Brando et al., 2010) or atmospheric aridity (Xu et al., 2017). Alternatively, leaf shedding in non-water-limited conditions may constitute an adaptive strategy to replace senescent leaves with efficient young leaves to maximize photosynthesis (Chen et al., 2020).*

Comment 20: L359-360: Should one of the "early wet season" be "dry season"?

Response: *Thank you for your comment. The "early wet season" contain a period of dry season rather than refer to the same period as the dry season. The "early wet season" refer to the transitional period between the end of the dry season and the beginning of the wet season.*

Comment 21: L397: Chen et al., 2019 is not found in the reference list.

Response: *Thank you for your attention to detail. "Chen et al., 2019" in caption of Figure 6 actually corresponds to this one in the reference list: Chen, X., Ciais, P.,*

Maignan, F., Zhang, Y., Bastos, A., Liu, L., Bacour, C., Fan, L., Gentine, P., Goll, D., Green, J., Kim, H., Li, L., Liu, Y., Peng, S., Tang, H., Viovy, N., Wigneron, J. P., Wu, J., Yuan, W., and Zhang, H.: Vapor Pressure Deficit and Sunlight Explain Seasonality of Leaf Phenology and Photosynthesis Across Amazonian Evergreen Broadleaved Forest, Global Biogeochemical Cycles, 35, 10.1029/2020gb006893, 2021. We have corrected the mistake cite in the revised version and checked and confirmed all the references.

Comment 22: L395: Is it possible to keep a consistent number of clusters between the three datasets? For example, can you set eight clusters in Lad-LAI, so the southeast Asia area has three clusters consistent with plots d-f. This will make it easier to compare the datasets.

Response: *Thank you for your constructive suggestion. We have updated the southeast Asia area to have three clusters consistent with plots d-f in Lad-LAI dataset, in order to make it easier to compare the datasets. The corresponding statistic figures has been updated accordingly.*
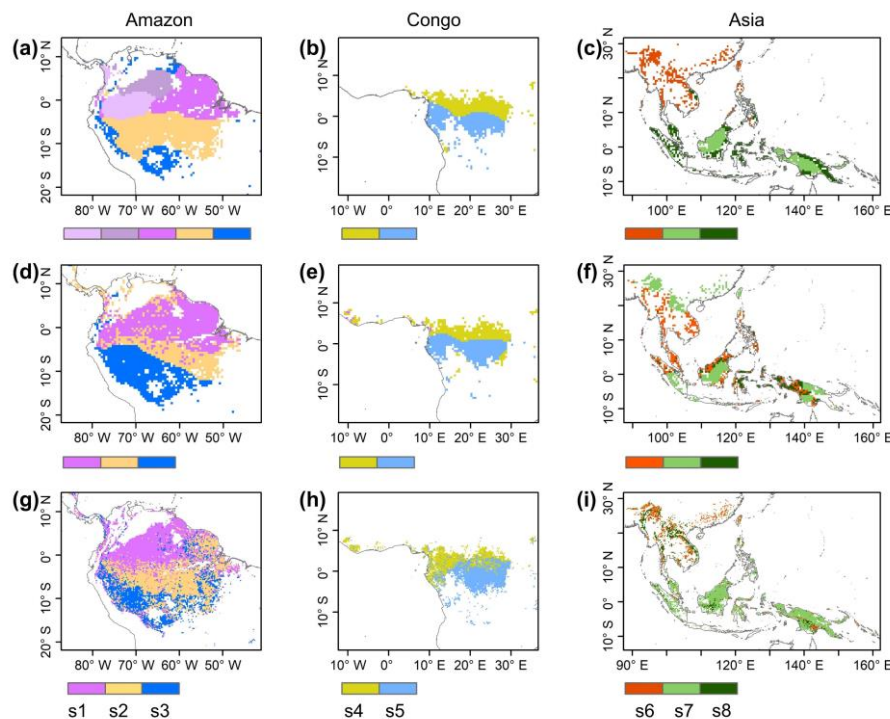

Figure 6. *Comparison of sub-regions of Lad-LAI products (plots g-i) with those of climatic factors classified by the K-means clustering analysis (plots a-c) (Chen et al., 2021) and those of the three climate-phenology regimes (plots d-f) developed by Yang et al. (2021).*
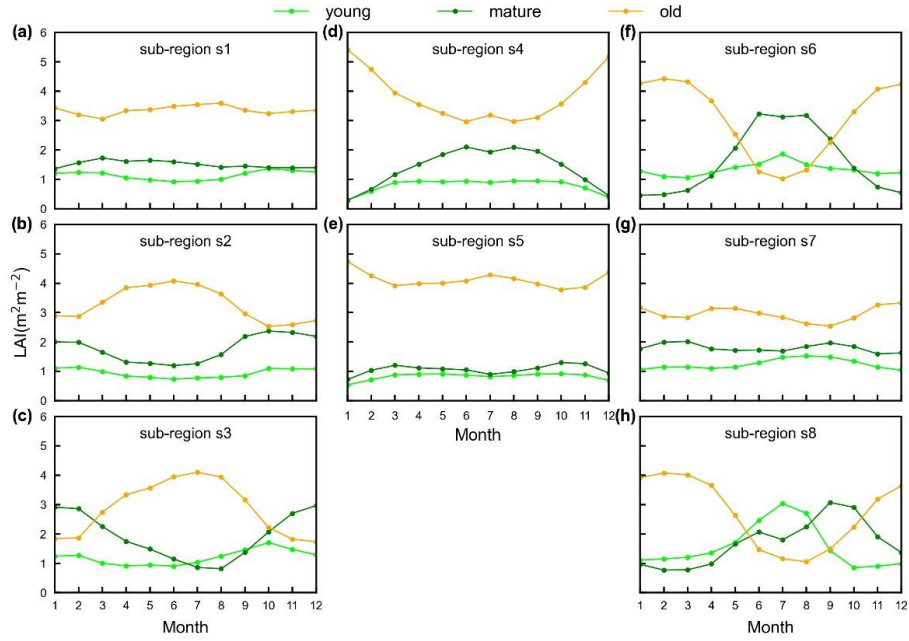
Figure 7. *Seasonality of simulated LAI$_{young}$, LAI$_{mature}$, and LAI$_{old}$ in 8 sub-regions classified by the K-means clustering analysis.*
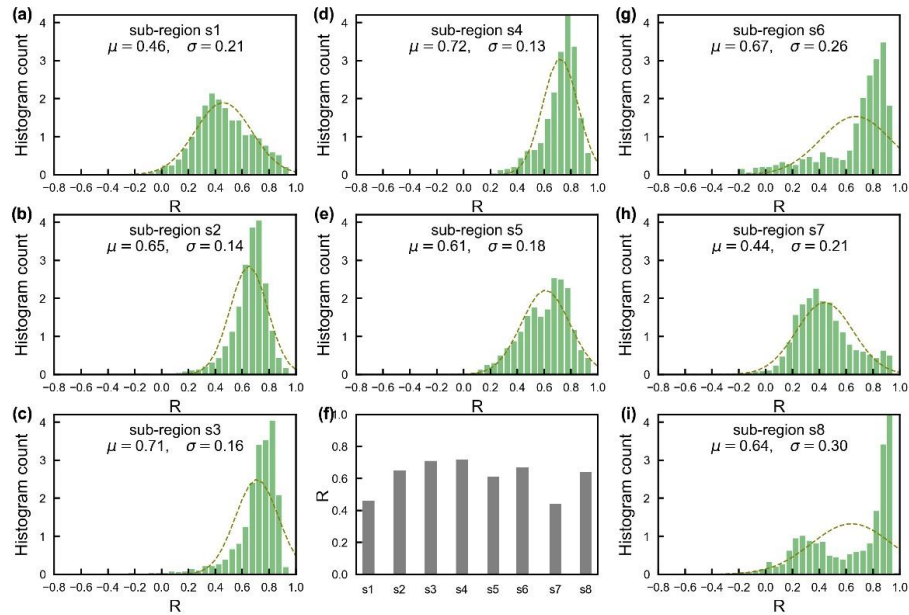

Figure 9. *Statistics of the Pearson correlation coefficient between seasonality of simulated LAI$_{young+mature}$ and MODIS Enhanced Vegetation Index (EVI) in the 8 clustered sub-regions. (a-e and g-i): the histogram of correlation coefficients; (f): mean of correlation coefficients in each sub-region*
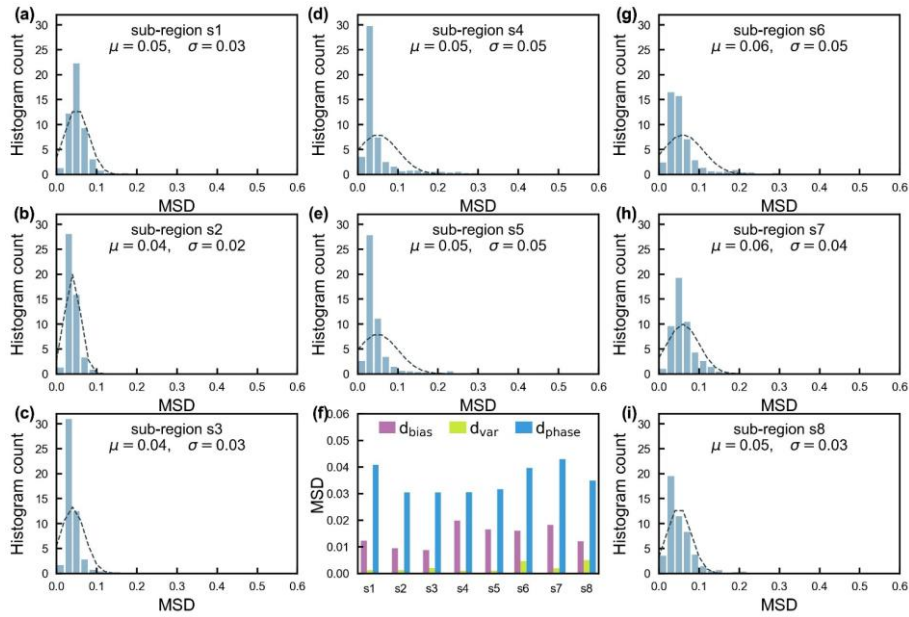
Figure 10. *Statistics of the Mean squared deviation (MSD) between seasonality of simulated LAI$_{young+mature}$ and MODIS Enhanced Vegetation Index (EVI) in the 8 clustered sub-regions. (a-e and g-i): the histogram of MSD; (f): mean of MSD in each sub-region.*

Comment 23: L413: I wonder if you have any hypothesis for the low performance in southeast Asia in comparison with other regions? (Figure 8a-c)

Response: *Yes. Compared to tropical evergreen forests of the Amazon and Africa, tropical Asian regions exhibit the lowest sensitivity of solar-induced chlorophyll fluorescence (SIF) (Guan et al., 2015; 2016).*

Comment 24: Figure 12: Please increase font size. It's not clear which line represents site data. Can you also illustrate the meaning of the dots?

Response: *Thank you for your comment. In the revised version, we have increased the font size of Figure 12 and added a legend to clarify which lines represent the site data. The orange dots in plots a-i represent the sharpest decreases day of old leaves and the black dots in plots a-i represent the peak day of litterfall mass. The black dots in plot j (right panel) represent the days when LAI$_{old}$ decreases sharpest (Day$_{LAIold}$) against the days when monthly litterfall peaks (Day$_{litterfall}$).*
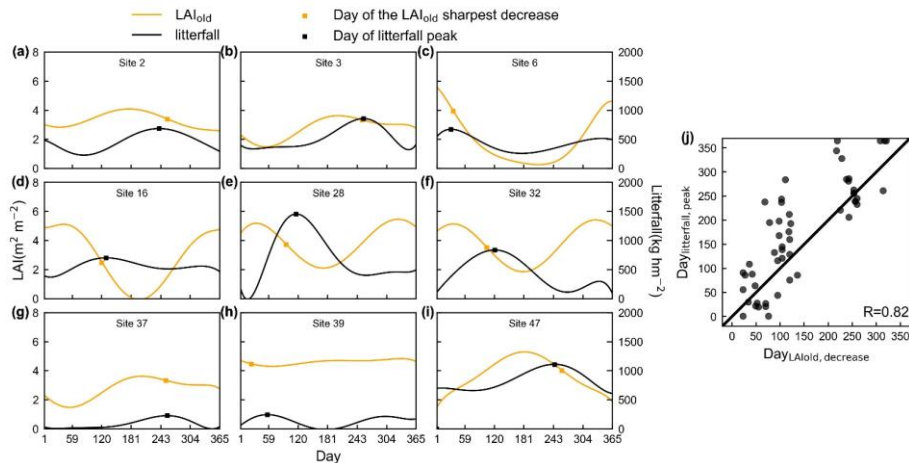
Figure 12. *Evaluation of simulated LAI_old using site-observed litterfall seasonality. (a-i) Days of a sharping decrease in LAI_old in comparison with days of corresponding litterfall peak at 9 specific sites for examples. The orange lines represent old leaves from simulation and dots represent the sharpest decrease day of old leaves. The black lines represent observed litterfall mass and dots represent the peak day of litterfall mass. (j) Comparisons of the days when LAI_old decreases sharpest (Day_LAIold) against the days when monthly litterfall peaks (Day_litterfall).*

Reference:

Asner, G.P., and Alencar, A.: Drought impacts on the Amazon forest: the remote sensing perspective. New Phytol. 187, 569–578. 2010.

Brando, P. M. et al. Seasonal and interannual variability of climate and vegetation indices across the Amazon. Proc. Natl Acad. Sci. USA, 107, 14685–14690. 2010

Chen, X., Huang, Y., Nie, C., Zhang, S., Wang, G., Chen, S., and Chen, Z.: A long-term reconstructed TROPOMI solar-induced fluorescence dataset using machine learning algorithms, Sci Data, 9, 427, 10.1038/s41597-022-01520-1, 2022.

Chen, X., Maignan, F., Viovy, N., Bastos, A., Goll, D., Wu, J., Liu, L., Yue, C., Peng, S., Yuan, W., Conceição, A. C., O'Sullivan, M., and Ciais, P.: Novel Representation of Leaf Phenology Improves Simulation of Amazonian Evergreen Forest Photosynthesis in a Land Surface Model, Journal of Advances in Modeling Earth Systems, 12, 10.1029/2018ms001565, 2020.

Chen, X., Ciais, P., Maignan, F., Zhang, Y., Bastos, A., Liu, L., Bacour, C., Fan, L., Gentine, P., Goll, D., Green, J., Kim, H., Li, L., Liu, Y., Peng, S., Tang, H., Viovy, N., Wigneron, J. P., Wu, J., Yuan, W., and Zhang, H.: Vapor Pressure Deficit and Sunlight Explain Seasonality of Leaf Phenology and Photosynthesis Across Amazonian Evergreen Broadleaved Forest, Global Biogeochemical Cycles, 35, 10.1029/2020gb006893, 2021.

de Moura, Y. M., Galvão, L. S., Hilker, T., Wu, J., Saleska, S., do Amaral, C. H., Nelson, B. W., Lopes, A. P., Wiedeman, K. K., Prohaska, N., de Oliveira, R. C., Machado, C. B., Luiz E.O.C. and Aragão.: Spectral analysis of amazon canopy phenology during the dry season using a tower hyperspectral camera and modis observations,

ISPRS Journal of Photogrammetry and Remote Sensing, 131, 52-64, https://doi.org/10.1016/j.isprsjprs.2017.07.006. 2017

Doughty, C. E. and Goulden, M. L.: Seasonal patterns of tropical forest leaf area index and CO_2 exchange. J. Geophys. Res. 113, G00B06. 2008.

Farquhar, G. D., von Caemmerer, S., and Berry, J. A.: A biochemical model of photosynthetic CO2 assimilation in leaves of C 3 species, Planta, 149, 78-90, 10.1007/BF00386231, 1980.

Galvão, L. S. et al. On intra-annual EVI variability in the dry season of tropical forest: a case study with MODIS and hyperspectral data. Remote Sens. Environ. 115, 2350–2359, 2011.

Guan, K., Berry, J. A., Zhang, Y., Joiner, J., Guanter, L., Huete, A. R., ... and Gentine, P.: Improving the monitoring of crop productivity using spaceborne solar-induced fluorescence. Global change biology, 22(2), 716-726. 2016.

Guan, K., Pan, M., Li, H., Wolf, A., Wu, J., Medvigy, D., Caylor, K. K., Sheffield, J., Wood, E. F., Malhi, Y., Liang, M., Kimball, J. S., Saleska, Scott R., Berry, J., Joiner, J., and Lyapustin, A. I.: Photosynthetic seasonality of global tropical forests constrained by hydroclimate, Nature Geoscience, 8, 284-289, 10.1038/ngeo2382, 2015.

Huete, A. R., Didan, K., Shimabukuro, Y. E., Ratana, P., Saleska, S. R., Hutyra, L. R., Yang, W., Nemani, R. R., and Myneni, R.: Amazon rainforests green-up with sunlight in dry season, Geophysical Research Letters, 33, 10.1029/2005gl025583, 2006.

Kikuzawa, K.: Leaf phenology as an optimal strategy for carbon gain in plants. Can. J. Bot. 73, 158–163. 1995.

Li, X., and Xiao, J.: Mapping photosynthesis solely from solar-induced chlorophyll fluorescence: A global, fine-resolution dataset of gross primary production derived from OCO-2. Remote Sensing, 11(21), 2563; https://doi.org/10.3390/rs11212563. 2019.

Melgosa, M., Huertas, R., and Berns, R. S.: Performance of recent advanced color-difference formulas using the standardized residual sum of squares index. Journal of the Optical Society of America A, 25(7), 1828-1834. https://doi.org/10.1364/JOSAA.25.001828. 2008

Melgosa, M., García, P. A., Gómez-Robledo, L., Shamey, R., Hinks, D., Cui, G., and Luo, M. R.: Notes on the application of the standardized residual sum of squares index for the assessment of intra- and inter-observer variability in color-difference experiments. Journal of the Optical Society of America A, 28(5), 949-953. https://doi.org/10.1364/JOSAA.28.000949. 2011

Myneni, R. B. et al. Large seasonal swings in leaf area of Amazon rainforests. Proc. Natl Acad. Sci. USA, 104, 4820–4823. 2007.

Saleska, S. R., Didan, K., Huete, A. R. and da Rocha, H. R.: Amazon forests green-up during 2005 drought. Science, 308, 612–612. 2007.

Toomey, M., Roberts, D. A. and Nelson, B.: The influence of epiphylls on remote sensing of humid forests. Remote Sens. Environ, 113, 1787–1798. 2009.

Vico, G., Thompson, S. E., Manzoni, S., Molini, A., Albertson, J. D., Almeida-Cortez, J.

S., Fay, P. A., Feng, X., Guswa, A. J., Liu, H., Wilson, T. G., and Porporato, A.: Climatic, ecophysiological, and phenological controls on plant ecohydrological strategies in seasonally dry ecosystems. Ecohydrol., 8, 658– 679. doi: 10.1002/eco.1533. 2015.

Xu, X., Medvigy, D., Joseph Wright, S., Kitajima, K., Wu, J., Albert, L. P., Martins, G. A., Saleska, S. R., and Pacala, S. W.: Variations of leaf longevity in tropical moist forests predicted by a trait-driven carbon optimality model, Ecol Lett, 20, 1097-1106, 10.1111/ele.12804, 2017.